Proceedings of the ASME 2014 Dynamic Systems and Control Conference
DSCC2014
October 22-24, 2014, San Antonio, TX, USA

DSCC2014-6275

A LOW-ORDER HCCI MODEL EXTENDED TO CAPTURE SI-HCCI MODE TRANSITION DATA WITH TWO-STAGE CAM SWITCHING

Patrick Gorzelic, Prasad Shingne,
Jason Martz, and Anna Stefanopoulou
University of Michigan
Ann Arbor, Michigan, 48109
Email: pgoz@umich.edu

Jeff Sterniak and Li Jiang
Robert Bosch LLC
Farmington Hills, Michigan, 48331

ABSTRACT

A low-order homogeneous charge compression ignition (HCCI) combustion model to support model-based control development for spark ignition (SI)/HCCI mode transitions is presented. Emphasis is placed on mode transition strategies wherein SI combustion is abruptly switched to recompression HCCI combustion through a change of the cam lift and opening of the throttle, as is often employed in studies utilizing two-stage cam switching devices. The model is parameterized to a steady-state dataset which considers throttled operation and significant air-fuel ratio variation, which are pertinent conditions to two-stage cam switching mode transition strategies. Inspection and simulation of transient SI to HCCI (SI-HCCI) mode transition data shows that the extreme conditions present when switching from SI to HCCI can cause significant prediction error in the combustion performance outputs even with the model's adequate steady-state fit. When a correction factor related to residual gas temperature is introduced to account for these extreme conditions, it is shown that the model reproduces transient performance output time histories in SI-HCCI mode transition data. The model is thus able to capture steady-state data as well as transient SI-HCCI mode transition data while maintaining a low-order cycle to cycle structure, making it tractable for model-based control of SI-HCCI mode transitions.

INTRODUCTION

Homogeneous charge compression ignition (HCCI) combustion offers significant improvements in fuel economy relative to traditional spark ignition (SI) gasoline combustion while producing low nitrogen oxide emissions [1]. An obstacle to attaining the benefits of HCCI is that its feasible operating range is limited to a low to mid speed-load region of the full regime of conventional engines. Outside this range, SI combustion must be reverted to, which implies that transitions between SI and HCCI combustion must carried out. Most SI/HCCI mode transition studies approach the problem by means of open-loop calibration of actuator sequences to change between the modes [2–11]. Other works have proposed model-based feedback control approaches [12, 13] to the mode transition problem, which may help alleviate the calibration burden associated with scheduling open-loop sequences and also improve robustness to operating condition and environmental factors.

A low-order, computationally efficient HCCI model is indispensable for model-based control approaches to SI/HCCI transitions, and may also be a useful tool for offline trajectory optimization in open-loop approaches. Numerous control-oriented HCCI models exist in the literature e.g. [14–19], though few are concerned with mode transitions. The models of [17, 18] utilize topologies wherein the model states evolve in the crank angle domain, and must be numerically integrated throughout the cycle to calculate performance outputs such as torque and combustion phasing. The higher fidelity and physicality of these models is preferable to reduce the dependency on empirical parameterization, however the implicit and complex relationship between the inputs and performance outputs present in such model topologies makes development of model-based controllers difficult. In [13], a linearized feedforward controller was designed based on a pre-

viously developed reduced order HCCI model [19], which was shown to improve performance during SI-HCCI mode transitions. The mode transition strategy employed in [13] differs from the strategies considered by this paper in that the mode is gradually changed from SI to HCCI through continuous phasing of the cams, while the strategies considered in this paper abruptly change the mode from SI to HCCI with a switch of the cam profile. The abrupt mode change results in a more drastic step in the operating condition when switching from SI to HCCI, which the model of this paper is modified to account for.

The purpose of this paper is to develop a simple three state cycle by cycle recompression HCCI combustion model which reproduces two-stage cam switching SI-HCCI mode transition data for use in mode transition control. Validation of the model in HCCI-SI direction is left for future work. The term cam switching specifies that the mode is changed between SI and HCCI through an abrupt switch of the cam profile which is coordinated with opening/closing of the throttle as in the strategies of [5–10]. Effort is made in the model development to accommodate HCCI engines with practical two-stage cam hardware, in that throttled HCCI conditions and a wide range of air-fuel ratio (AFR) conditions are considered in the steady-state parameterization. These conditions are pertinent to two-stage cam engines due to the impracticality of fully dethrottling the SI combustion at constant load for switching to/from HCCI. This is in contrast to more costly variable valve actuation systems wherein the cylinder breathing can be controlled through the flexible valve train with a fully dethrottled intake as in [2–4, 18]. The model is evaluated against experimental open-loop SI-HCCI mode transition data, which shows that the extreme conditions when switching from SI to HCCI can still produce significant errors despite the model's notable steady-state validity. When an additional correction is introduced to capture these conditions, the model is able to reproduce SI-HCCI performance output time histories well. The conditions considered for SI-HCCI transitions correspond to two different load points at an engine speed of 2000 RPM, which are depicted in a representative speed-load map in Fig. 1. The major operating variable differences between SI and HCCI at these points is also shown, where the symbols NMEP, EVC, IVO, p_{im}, T_{exh} refer to net indicated mean effective pressure, exhaust valve closing timing, intake valve opening timing, intake manifold pressure, and exhaust runner temperature, respectively.

The paper first summarizes a baseline steady-state model taken from [16] and describes the most important modifications and new features that were necessary to capture the range of steady-state conditions considered. A description of the steady-state parameterization data along with the model reproduction of the outputs in the data follows. SI-HCCI mode transition data and evaluation of the model in SI-HCCI transients is then discussed, which motivates the introduction of a mode transition correction factor. The paper concludes with a summary of the important model aspects.

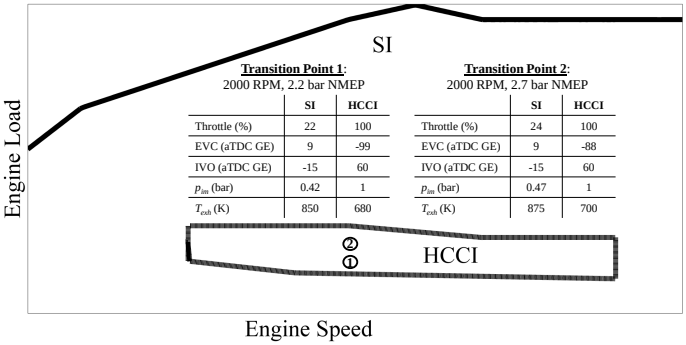

FIGURE 1. Representative speed-load map showing SI/HCCI regions and the operating points considered in SI-HCCI transition experiments.

STEADY-STATE HCCI MODELING

Model Overview

The HCCI model in this paper is developed starting from [16] as a baseline. The model operates on a discrete cycle to cycle time scale where the cycle division is drawn at exhaust valve opening (EVO), with states that are passed between cycles to capture cyclic thermal and compositional couplings. The model is based on simple relations for polytropic compression and expansion processes and instantaneous combustion combined with an integrated Arrhenius rate for combustion phasing and regressions for other in-cylinder quantities.

Multiple modifications and new features were necessary to extend the base model's steady-state validity to conditions that were considered for SI-HCCI mode transitions, mostly concerned with the effects of throttled conditions and AFRs that varied from stoichiometric or rich to very lean. The most major changes are briefly described below.

The state description is extended to include the mass fraction of unburnt fuel at the blowdown event f_{bd} in addition to the blowdown temperature T_{bd} and burned gas fraction b_{bd}. The f_{bd} state captures recycled fuel from rich combustion and also enables the incorporation of recompression heat release effects which will be discussed shortly. The Arrhenius threshold for start of combustion is modified with dependencies for recompression AFR and temperature, which are intended to capture how these variables influence recompression reactions which go onto affect fuel ignitability. These dependencies are incorporated via the Arrhenius threshold following the logic in [20]. Without these dependencies, fits to combustion phasing data were poor even when multiple correlations from the literature [14,19,21,22] were tried. The form of the function is based on observations from [23], which found that an optimum point for advancing combustion phasing via recompression reaction was achieved at intermediate AFRs where a balance was struck between ignitability enhancing pyrolysis reactions and ignitability inhibiting fuel reformation reactions. A combined thermal and combustion efficiency term is

introduced as a function of the in-cylinder relative AFR λ_c to account for changes in work output as AFR is varied by adjusting the temperature and hence pressure rise due to combustion. The efficiency term represents mainly the effects of combustion efficiency as λ_c nears stoichiometry and more the effect of thermal efficiency as λ_c becomes significantly lean. In addition to these changes to expand the model's validity, the cylinder breathing model was reformulated to include a regression for the residual mass m_r as opposed to the residual gas fraction x_r, which proved favorable for extension to mode transition transients.

Recompression heat release (RCHR) of recycled unburnt fuel from main combustion was apparent in SI-HCCI mode transition data where cycles with late combustion phasing were followed by an enlarged recompression peak. The resulting cycle to cycle coupling that is explained in [24] is captured with a model modified after that in [25], which consists of a sigmoidal main combustion efficiency to capture unburnt fuel at late combustion phasing, and an instantaneous combustion of the unburnt fuel at a fixed angle during recompression. The combustion efficiency is parameterized as a function of the 50% burn angle θ_{50} whose sigmoidal roll-off varies with fuel mass m_f to capture changes in the late phasing limit with load. The instantaneous combustion of the unburnt fuel is simplified from that in [25] in that it is taken to occur with 100% efficiency directly at EVC. The heat release was chosen to be at EVC because this conforms with the rest of model structure and aids the model regression.

Several of the important steady-state model aspects are exemplified in the throttle sweep data shown in Fig. 2. All other inputs are held constant and the data is plotted versus p_{im}. As the throttle is closed (moving right to left), the θ_{50} at first advances and then retards, which is interpreted to be a consequence of trade-offs between temperature and pressure effects on auto-ignition as well as chemical effects on recompression reactions due to varying oxygen concentration during recompression. Definitively characterizing the relative magnitudes of these effects on combustion is a difficult task for which work is still ongoing, however the model is able to reproduce the qualitative trend as well as approximate the absolute values of θ_{50} with sufficient accuracy. The plot of gross indicated mean effective pressure (IMEP) illustrates the trend for which the combined thermal and combustion efficiency is incorporated. As can be seen, as the throttle is closed and λ decreases, there is at first a mild reduction in the work output from combustion, which becomes more severe as stoichiometry is approached. Note that IMEP is shown as opposed to NMEP to exclude any effects of pumping work.

Steady-State Fitting Results

The test engine to which the model is parameterized is a four cylinder, two liter displacement engine with a geometric compression ratio of 11.7:1. The model is parameterized to a single cylinder of the four. The engine is equipped with a two-stage

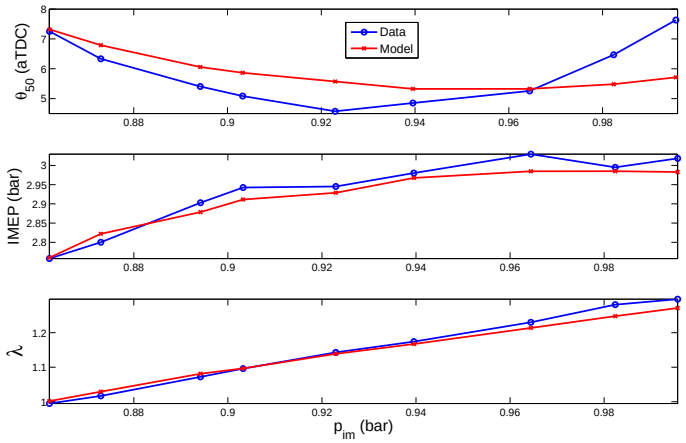

FIGURE 2. Sweeps of throttle with all other inputs held fixed at 2000 RPM. Model reproduction of data is shown.

cam system to switch between high/low lift cams for SI/HCCI operation and intake and exhaust cam phasers to vary the valve timings, similar to the configurations of [6–10]. The high lift and low lift cams are offset from each other by a fixed crank angle amount, so that when the cams are switched, the valve timings change instantaneously. This offset is characterized by the difference in the IVO and EVC for the intake and exhaust cams which are equal to 47° and -34°, respectively.

The dataset to which the model is parameterized consists of a 526 point grid of actuator sweeps at a single engine speed of 2000 RPM with the outermost swept variable being fuel mass m_f, followed p_{im} (adjusted via throttle) and then EVC timing θ_{evc}, and the innermost variable being injection timing θ_{soi}. Several direct throttle and EVC sweeps were also carried out to clearly discern the trend in the outputs with respect to these variables. Intake valve timing was held fixed with intake valve closing (IVC) near BDC, as it was observed to have only a small effect on combustion in the vicinity of BDC. The grid of inputs and corresponding performance outputs of θ_{50}, NMEP, and λ are shown in Fig. 3.

The model parameters were regressed using an iterative parameterization routine to consider the model's inherent internal feedback, and the reproduction of the performance outputs is plotted against the data in Fig. 3. As can be seen, the model reproduces the performance outputs with good accuracy for a low-order model considering the wide range of actuator settings over which it is fit. A summary of the swept input and output range and mean and max absolute model errors is given in Table 1.

EXTENSION TO SI-HCCI MODE TRANSITIONS

This Section discusses results from an experimental open-loop SI-HCCI mode transition and describes modifications to the base model needed to accurately capture the mode transition.

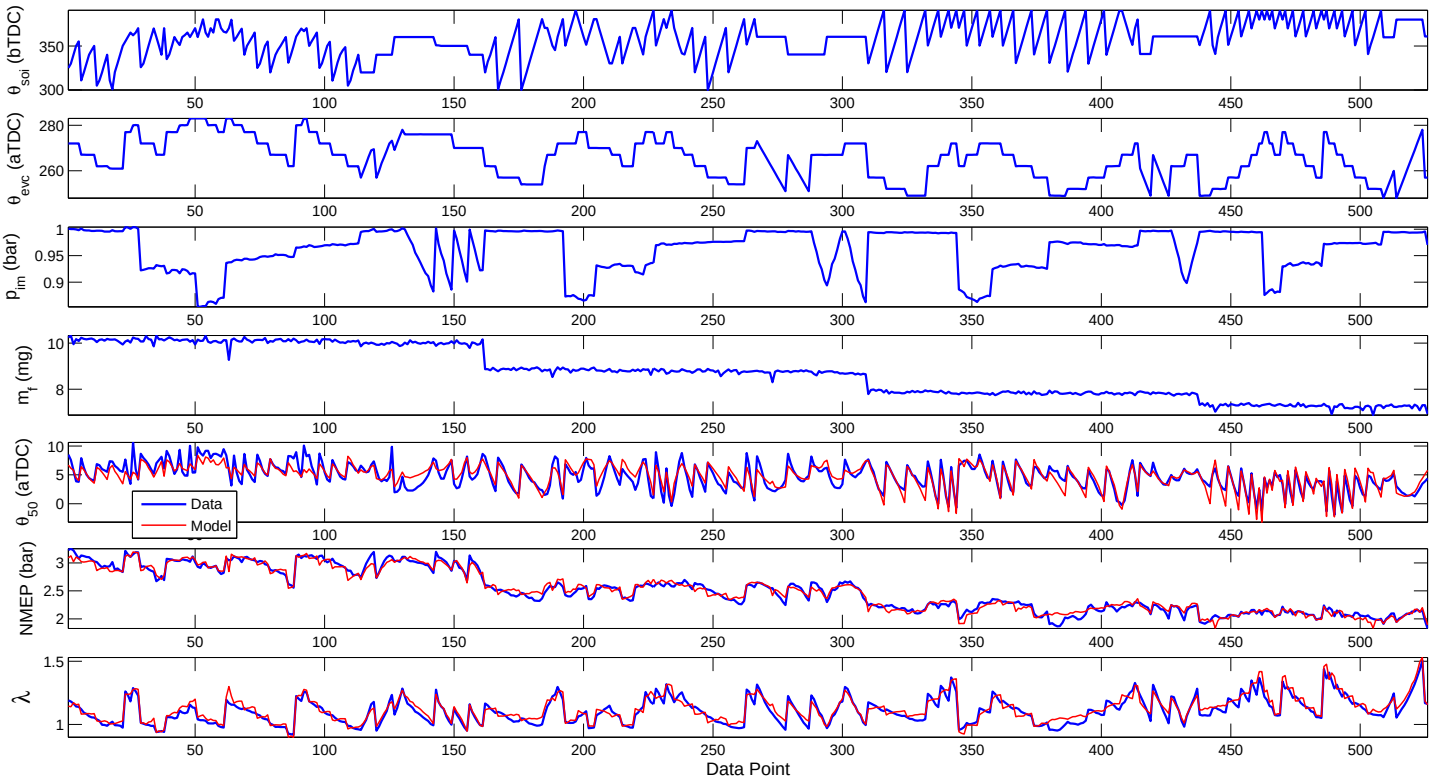

FIGURE 3. Input grid and modeled vs. measured outputs for steady-state model parameterization data.

	Min	Max	Mean Abs. Err.	Max Err.
θ_{soi} (bTDC)	300	390	-	-
θ_{evc} (aTDC)	250	290	-	-
p_{im} (bar)	0.85	1	-	-
m_f (mg)	7.2	10.5	-	-
θ_{50} (aTDC)	-2	11	0.86°	5.16°
$NMEP$ (bar)	1.7	3	2.06%	12.2%
λ	0.92	1.5	2.81%	11.2%

TABLE 1. Swept range of inputs and outputs in HCCI model parameterization data. Mean and max absolute error between model and measurement listed for outputs. θ_{50} error reported in CAD to avoid division by small numbers at θ_{50} near TDC.

Mode Transition Overview

The format for the mode transition experiments was to take the engine to a steady-state condition in SI mode which was appropriate for switching to HCCI, then to switch the intake and exhaust cams simultaneously. The cams switch while the valves are closed during the final SI cycle. The SI switch point condition was set with an advanced EVC and retarded IVO timing in order to diminish cylinder breathing as throttle was opened in an attempt to maintain constant load while dethrottling. The throttle was commanded open roughly 20-30 milliseconds before the first low-lift cam breathing event. In the simulation results presented along with the data, the HCCI model is initialized with estimates of the model states taken from steady-state data at the SI switch point. The mode transition discussed corresponds to transition point 1 in Fig. 1 for which the initial conditions for the first HCCI cycle are estimated to be $[T_{bd}^0, b_{bd}^0, f_{bd}^0] = [960\text{ K}, 0.893, 0]$, where superscript ^{0} indicates a recycled state from the previous cycle. T_{bd}^0 is estimated based on exhaust runner temperature and b_{bd}^0 and f_{bd}^0 are calculated using the AFR on the final SI cycle which was commanded to $\lambda = 1.18$. The values of 0 for f_{bd}^0 and 0.893 for b_{bd}^0 indicate that approximately 10.7% of the residual charge consists of unburnt air with no unburnt fuel.

The combustion response and corresponding input sequences for the SI-HCCI mode transition trial are shown in Fig. 4, where *SI -1* and *HCCI 0* designate the final SI cycle and first HCCI cycle, respectively, following the notation in [18]. The slight recompression peak in cycle *SI -2* is the result of the early EVC and late IVO timing at the SI end point employed to assist in dethrottling the engine. The independent axis of the time-

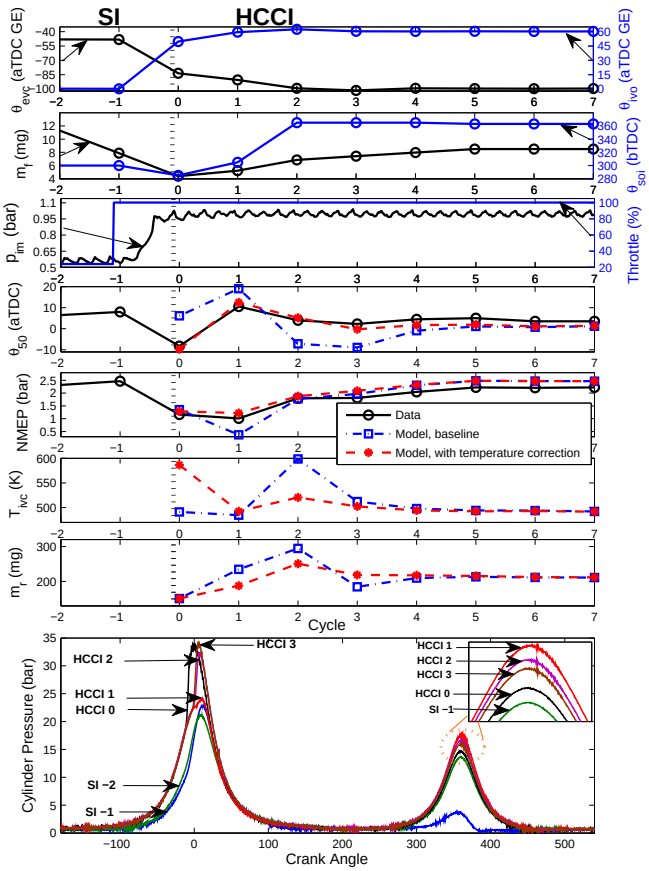

FIGURE 4. Cycle by cycle input and outputs and crank angle resolved in-cylinder pressure during open-loop SI-HCCI mode transition at transition point 1 defined in Fig. 1. *SI -1* indicates final SI cycle and *HCCI 0* indicates first HCCI cycle. Model reproduction of outputs with and without the introduced residual temperature correction are shown.

based signals of intake manifold pressure and throttle command is transformed in order to plot these variables against engine cycle. The cams switch from high to low lift during the closed-valve portion of cycle *SI -1*, so that the following recompression peak is much larger. The sudden jump of the valve timings θ_{evc} and θ_{ivo} at cycle *HCCI 0* corresponds to this switch. In anticipation of the high exhaust temperature that is carried over from the final SI cycle, both the θ_{evc} and θ_{soi} timings are placed much later than their steady-state set points when HCCI is entered to retard combustion phasing. However, on cycle *HCCI 0*, the combustion phasing is still early, accompanied by a high pressure rise rate. The combustion phasing then shifts later on cycle *HCCI 1* where the exhaust temperature is now the result of HCCI combustion and so is significantly lower. This initial early combustion phasing which then moves later due to the cycle to cycle temperature coupling is the same phenomenon observed in the mode transition portrayed in [18]. Following the late combustion phasing and weak heat release on the cycle *HCCI 1*, the recompression event exhibits an enlarged peak pressure which occurs significantly after TDC, which indicates RCHR of unburnt fuel from the main combustion event. This RCHR in conjunction with the earlier injection timing cause the combustion phasing to advance on cycle *HCCI 2*, and from here the transient becomes milder and the combustion settles to steady-state.

Baseline Model Response During SI-HCCI Transition

As is apparent from the dash-dot θ_{50} response in Fig. 4, the baseline model does not capture the extremely advanced combustion phasing on cycle *HCCI 0*. This is unexpected, given that the model fits a large steady-state dataset with good accuracy (see Fig. 3), and contains blowdown temperature dynamics to capture the thermal coupling from the recycled SI exhaust gas. Significant phasing errors occur on the cycles following *HCCI 0* as well, which may be related to this large initial error through the cycle to cycle coupling. The plot of the model predicted in-cylinder temperature at IVC T_{ivc} shows that the baseline model predicts a T_{ivc} value on cycle *HCCI 0* which is similar to the value at cycles *HCCI 6*, *HCCI 7*. This result is not intuitive, as the high exhaust temperature that is carried over from SI on cycle *HCCI 0* should be expected to yield to a T_{ivc} value that is significantly greater than in the cycles towards the end of the transition where the transient effects of the SI exhaust temperature have settled out. If T_{ivc} is under predicted, it could be responsible for the late θ_{50} prediction on cycle *HCCI 0*.

When interpreting the model's T_{ivc} predictions on cycle *HCCI 0*, it is important to consider that the conditions on this cycle are well outside the envelope of steady-state HCCI operation to which the model is parameterized. This large excursion from the model's nominal fitting range may increase the model's prediction error relative to the steady-state fit, which has the potential to result in large T_{ivc} errors. The most obvious variable which may contribute to this error is the exhaust temperature, which is estimated to be over 250 K higher than the nominal HCCI value at the given fueling and so induces a high degree of extrapolation. Additionally, the inputs to the model are set at extreme values which would otherwise be infeasible at steady-state in order to compensate for this high exhaust temperature, most notably in that the EVC timing is 17° later than the steady-state set point. The late EVC timing compounds with the high exhaust temperature to yield a very low trapped residual mass on cycle *HCCI 0*, as can be observed in Fig. 4. The reduced residual mass presents a competing effect with the high exhaust temperature on the cylinder charge after intake, in that it acts to reduce the residual internal energy while the high exhaust temperature acts to increase it. Capturing the net outcome of these competing effects further complicates the problem of extrapolation on cycle *HCCI 0*. Fig. 4 also shows that the intake pressure goes through a sharp transient leading into cycle *HCCI 0*, rising from roughly

0.55 to 1 bar in approximately 20 milliseconds. This sharp transient may perturb the inducted air charge relative to what would otherwise be present at steady-state with the given intake pressure, which will go onto affect the in-cylinder temperature. To gain a better understanding of these effects on cycle *HCCI 0* and deduce whether the model's θ_{50} error on cycle *HCCI 0* stems from error in it's predicted T_{ivc}, a crank-angle based simulation of the SI-HCCI mode transition is presented next.

Mode Transition Predictions Using Crank-Angle Based Model

For a higher fidelity estimate of the in-cylinder dynamics during the SI-HCCI mode transition from which to draw conclusions about the source of model error, a simplified single-cylinder GT-Power simulation was carried out. Measured intake and exhaust manifold pressures and temperatures were specified as intake and exhaust runner boundary conditions on a crank angle basis, and the valve profiles/timings from the experiment were imposed to capture the effect of the cam switch from high to low lift and rapid cam phasing. To validate the GT-Power simulation, the experimental pressure traces are compared versus those generated by the simulation in Fig. 5. The GT-Power simulation matches experiment with satisfactory accuracy which indicates that its predictions should be reasonable.

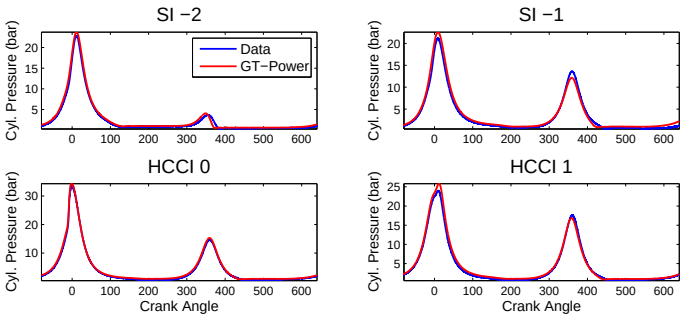

FIGURE 5. Comparison of experimental versus GT-Power simulation in-cylinder pressure during an SI-HCCI mode transition.

Inspection of the GT-Power simulation results suggested that for the HCCI model of this paper, the dominant factor contributing to prediction error when switching from SI to HCCI is related to the effect of the high SI exhaust temperature on the residual gas temperature leading into the *HCCI 0* cycle. Fig. 6 plots consecutive in-cylinder temperature traces calculated by GT-Power during the mode switch from SI to HCCI. There is a clear trend that on cycle *HCCI 0*, the temperature at the end of recompression is 200 - 300 K higher than the remainder of the HCCI cycles, which goes onto yield a significantly higher temperature after the intake event. This is in contrast with the negligible difference in

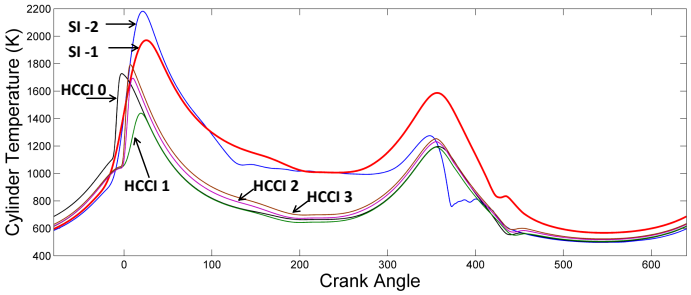

FIGURE 6. In-cylinder temperature traces generated by GT-Power SI-HCCI mode transition simulation. The final SI cycle whose recompression event yields an extremely high temperature leading into the first HCCI cycle is highlighted.

the in-cylinder temperature on cycle *HCCI 0* from steady-state predicted by the HCCI model in Fig. 4.

Residual Temperature Correction for Initial HCCI Cycle

Based on the observations from Figs. 4, 6, the model's prediction error when entering HCCI is attributed to its extrapolation to the high exhaust temperature that is carried over from SI, and so the error is taken to be restricted to the first HCCI cycle after which the conditions should become much closer to the nominal HCCI range. A correction factor is introduced into the model's prediction of the residual gas temperature T_r, because T_r couples the recycled blowdown temperature state to the in-cylinder mass and temperature at IVC through an energy balance type expression similar to [16], and is fit only to steady-state data. The correction takes the form a scaling coefficient on T_r, denoted k_r, which is applied only on the first HCCI cycle. In parameterization, k_r is regressed to match combustion phasing when HCCI is switched into, as combustion phasing is the most pertinent variable for determining k_r for which a measurement is available in SI-HCCI transients; instrumentation or post-processing tools to determine other related variables such as the in-cylinder temperature or inducted air charge during the transient were not available. For the mode transition trial here, $k_r \equiv 1.208$, corresponding to inflating the steady-state model's residual temperature prediction by 20.8%.

With the introduction of the residual temperature correction, the T_{ivc} predicted by the model on the cycle *HCCI 0* in Fig. 4 is increased relative to its steady-state value, following the trend observed in the GT-Power simulation. The temperature rise due to RCHR on cycle *HCCI 2* is now more reasonable as well. The θ_{50} response predicted by the model in Fig. 4 (dashed line) now matches the data well not only on cycle *HCCI 0* where the correction is applied, but for the entire transient process. This indicates that the main effect driving the erroneous transient response predicted by the nominal model is the error induced by the extreme conditions on the cycle *HCCI 0*, which goes onto affect subse-

quent cycles though the cycle to cycle states. Once this error is corrected for, the nominal model can capture the remainder of the transient response, as the conditions become much closer to the nominal HCCI range. Throughout the transient, the model is able to capture the effects of varying fuel quantity, injection timing, EVC timing, as well as any variations in AFR due to rapid changes in these actuators.

Validation with a Different SI-HCCI Transition Sequence

To corroborate the modeling approach, the model is exercised to simulate a mode transition sequence at transition point 2 defined in Fig. 1. This represents a transition an operating point that is approximately 0.5 bar NMEP higher than the case previously considered, or roughly 25% of the HCCI load range at 2000 RPM on the experimental engine. The initial conditions for the first HCCI cycle at this operating condition are estimated to be $[T^0_{bd}, b^0_{bd}, f^0_{bd}] = [980\text{ K}, 0.823, 0]$, where the only slightly higher blowdown temperature estimate is the result of a leaner mixture on the final SI cycle where $\lambda = 1.3$. The model parameters, including the residual temperature correction k_r, are unchanged from the their values at transition point 1. The model predictions of the performance outputs θ_{50} and NMEP along with the important combustion inputs are plotted in Fig. 7. Again it can be seen the model reproduces the combustion outputs well. The ability of the model to reproduce this alternate SI-HCCI mode transition without adjusting the k_r value may suggest that k_r has only a mild sensitivity to operating condition. However, to definitively determine the degree of variation and potential regression/tabulation of k_r versus operation condition, more SI-HCCI transition data over a wider range of conditions are necessary.

CONCLUSIONS

A low-order HCCI combustion model extended to capture SI-HCCI mode transition data with two-stage cam switching strategies has been presented. The model was shown to fit steady-state data over a wide range of conditions, including throttled HCCI and rich to very lean AFRs which may be encountered in two-stage cam switching mode transitions strategies. Despite the adequate steady-state accuracy, the model's predicted response exhibited significant error when simulated with SI-HCCI mode transition data. The origin of of this error was traced to the extreme conditions on the first HCCI cycle when switching from SI to HCCI, which are well outside the nominal HCCI operating range. The dominant factor contributing to the prediction error was found to be related to the high exhaust temperature that is carried over from SI, and so a correction factor which accounts for the error through the residual gas temperature was introduced. With the correction factor in place, the model reproduced transient performance output time histories well for two

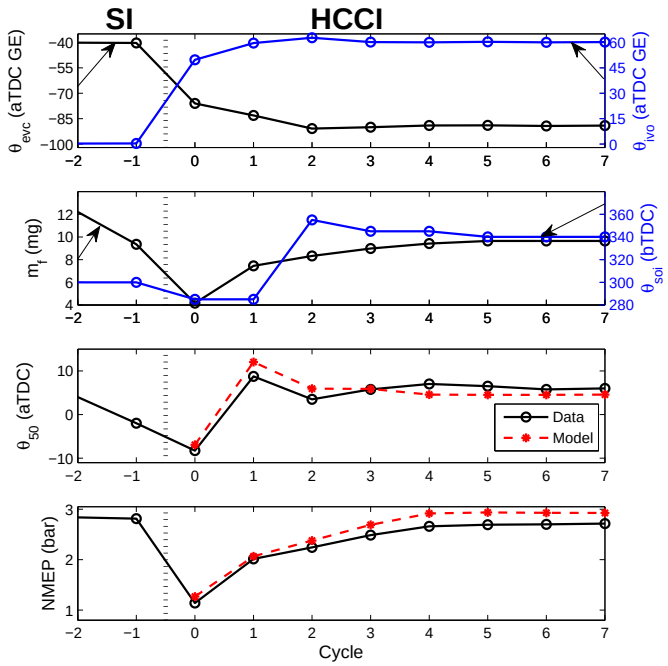

FIGURE 7. SI-HCCI mode transition simulation at transition point 2 defined in Fig. 1. Steady-state model parameters and SI-HCCI residual temperature correction factor are unchanged from transition point 1.

different SI-HCCI mode transition sequences.

Further investigation of the in-cylinder phenomena when switching from SI to HCCI and evaluation of the proposed residual gas temperature correction method over a wider range of SI-HCCI transitions is planned for future work. Additionally, extension of the low-order HCCI modeling approach of this paper to encompass the effects of spark assist is a pertinent topic for future research, as many mode transition studies [4,5,7,9,11,26] have found spark assist to be helpful.

ACKNOWLEDGMENT

This material is based upon work supported by the Department of Energy [National Energy Technology Laboratory] under Award Number(s) DE-EE0003533. [1] This work is performed as a part of the ACCESS project consortium (Robert Bosch LLC, AVL Inc., Emitec Inc., Stanford University, University of Michi-

[1]Disclaimer: This report was prepared as an account of work sponsored by an agency of the United States Government. Neither the United States Government nor any agency thereof, nor any of their employees, makes any warranty, express or implied, or assumes any legal liability or responsibility for the accuracy, completeness, or usefulness of any information, apparatus, product, or process disclosed, or represents that its use would not infringe privately owned rights. Reference herein to any specific commercial product, process, or service by trade name, trademark, manufacturer, or otherwise does not necessarily constitute or imply its endorsement, recommendation, or favoring by the United States Government or any agency thereof. The views and opinions of authors expressed herein do not necessarily state or reflect those of the United States Government or any agency thereof.

gan) under the direction of PI Hakan Yilmaz and Co-PI Oliver Miersch-Wiemers, Robert Bosch LLC.

NOMENCLATURE

bTDC/aTDC before/after Top Dead Center
IVO/IVC Intake Valve Opening/Closing timing
EVO/EVC Exhaust Valve Opening/Closing timing
RCHR Recompression Heat Release
AFR Air-Fuel Ratio
λ/λ_c Relative AFR in the exhaust/cylinder
T_{bd} Temperature after blowdown
b_{bd} Burned gas fraction after blowdown
f_{bd} Unburnt fuel mass fraction after blowdown
m_f Fuel mass
m_r Residual mass
θ_{50} Crank angle of 50% mass fraction burned
p_{im} Pressure in intake manifold
NMEP/IMEP Net/Gross Indicated Mean Effective Pressure
$\theta_{ivo}/\theta_{evc}$ Cam phaser IVO/EVC position
θ_{soi} Start of fuel injection timing
k_r Residual gas temperature correction for SI-HCCI transition

References

[1] Zhao, F., Asmus, T., Assanis, D., Dec, J., Eng, J., and Najt, P., 2003. *Homogeneous Charge Compression Ignition (HCCI) Engines: Key Research and Development Issues*. SAE International.

[2] Koopmans, L., Ström, H., Lundgren, S., Backlund, O., and Denbratt, I. "Demonstrating a SI-HCCI-SI mode change on a Volvo 5-cylinder electronic valve control engine". *SAE Technical Paper 2003-01-0753*.

[3] Santoso, H., Matthews, J., and Cheng, W. "Managing SI/HCCI dual-mode engine operation". *SAE Technical Paper 2005-01-0162*.

[4] Zhang, Y., Xie, H., Zhou, N., Chen, T., and Zhao, H. "Study of SI-HCCI-SI transition on a port fuel injection engine equipped with 4VVAS". *SAE Technical Paper 2007-01-0199*.

[5] Milovanovic, N., Blundell, D., Gedge, S., and Turner, J. "SI-HCCI-SI mode transition at different engine operating conditions". *SAE Technical Paper 2005-01-0156*.

[6] Tian, G., Wang, Z., Ge, Q., Wang, J., and Shuai, S., 2007. "Control of a spark ignition homogeneous charge compression ignition mode transition on a gasoline direct injection engine". *Proceedings of the Institution of Mechanical Engineers, Part D: Journal of Automobile Engineering,* ***221***(867).

[7] Cairns, A., and Blaxill, H. "The effects of two-stage cam profile switching and external EGR on SI-CAI combustion transitions". *SAE Technical Paper 2007-01-0187*.

[8] Kalian, N., Zhao, H., and Qiao, J., 2008. "Investigation of transition between spark ignition and controlled auto-ignition combustion in a v6 direct-injection engine with cam profile switching". *Proc. of the Institution of Mech. Engineers, Part D: J. Automobile Engineering,* ***222***, pp. 1911–1926.

[9] Wu, H., Collings, N., Regitz, S., Etheridge, J., and Kraft, M. "Experimental investigation of a control method for SI-HCCI-SI transition in a multi-cylinder gasoline engine". *SAE Technical Paper 2010-01-1245*.

[10] Nier, T., Kulzer, A., and Karrelmeyer, R. "Analysis of the combustion mode switch between SI and gasoline HCCI". *SAE Technical Paper 2012-01-1105*.

[11] Kakuya, H., Yamaoka, S., Kumano, K., and Sato, S. "Investigation of a SI-HCCI combustion switching control method in a multi-cylinder gasoline engine". *SAE Technical Paper 2008-01-0792*.

[12] Gorzelic, P., Hellström, E., Stefanopoulou, A., and Jiang, L., 2012. "Model-based feedback control for an automated transfer out of SI operating during SI to HCCI transitions in gasoline engines". ASME Dynamic Systems and Control Conference.

[13] Ravi, N., Jagsch, M., Oudart, J., Chaturvedi, N., Cook, D., and Kojic, A., 2013. "Closed-loop control of SI-HCCI mode switch using fuel injection timing". ASME Dynamic Systems and Control Conference.

[14] Shaver, G., Gerdes, J., Roelle, M., Caton, P., and Edwards, C., 2005. "Dynamic modeling of residual-affected homogeneous charge compression ignition engines with variable valve actuation". *J. Dyn. Sys. Meas. Control,* ***127***(3), pp. 374–81.

[15] Rausen, D., Stefanopoulou, A., Kang, J., Eng, J., and Kuo, T., 2005. "A mean value model for control of homogeneous charge compression ignition (HCCI) engines". *J. Dyn. Syst. Meas. Control,* ***127***(3), pp. 355–362.

[16] Jade, S., Hellström, E., Larimore, J., Stefanopoulou, A., and Jiang, L., To appear. "Reference governor for load control in a multicylinder recompression HCCI engine". *IEEE Trans. Control Sys. Tech.*

[17] Yang, X., and Zhu, G., 2011. "A two-zone control oriented SI-HCCI hybrid combustion model for the HIL engine simulation". IEEE American Control Conference.

[18] Shaver, G., Roelle, M., and Gerdes, J., 2006. "Modeling cycle-to-cycle dynamics and mode transition in HCCI engines with variable valve actuation". *Control Engineering Practice,* ***14***, pp. 213–222.

[19] Ravi, N., Roelle, M., Liao, H., Jungkunz, A., Chang, C., Park, S., and Gerdes, J., 2010. "Model-based control of HCCI engines using exhaust recompression". *IEEE Trans. Control Sys. Tech.,* ***18***(6), pp. 1289–1302.

[20] Ravi, N., Liao, H.-H., Jungkunz, A., Chang, C.-F., Song, H., and Gerdes, J., 2012. "Modeling and control of an exhaust recompression HCCI engine using split injection". *J. Dyn. Syst. Meas. Control,* ***134***, pp. 231–250.

[21] Yun, H., Guralp, O., Grover, R., and Najt, P., 2013. "The effect of temperature and oxygen concentration on auto-ignition at low-load operating conditions in a gasoline homogeneous charge compression ignition engine". *Int. J. Engine Research,* ***14***(5), pp. 512–524.

[22] He, X., Donovan, M., Zigler, B., Palmer, T., Walton, S., Woolridge, M., and Atreya, A., 2005. "An experimental and modeling study of iso-octane ignition delay times under homogeneous charge compression ignition conditions". *Combustion and Flame,* ***142***, pp. 266–275.

[23] Song, H. H., and Edwards, C. F., 2009. "Understanding chemical effects in low-load-limit extension of homogeneous charge compression ignition engines via recompression reaction". *Int. J. Engine Research,* ***10***, pp. 231–250.

[24] Hellström, E., Larimore, L., Stefanopoulou, A., Sterniak, J., and Jiang, L., 2012. "Quantifying cyclic variabilityin a multicylinder HCCI engine with high residuals". *J. Eng. for Gas Turb. and Power,* ***134***(11), pp. 112803–1–8.

[25] Hellström, E., and Stefanopoulou, A., 2011. "Modeling cyclic dispersion in autoignition combustion". IEEE Conference on Decision and Control.

[26] Matsuda, T., Wada, H., Kono, T., Nakamura, T., and Urushihara, T. "A study of a gasoline-fueled HCCI engine mode changes from SI combustion to HCCI combustion". *SAE Technical Paper 2008-01-0050*.